HOSTED BY

ELSEVIER

Available online at www.sciencedirect.com

ScienceDirect

journal homepage: www.elsevier.com/locate/bjbas

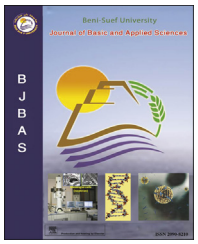

Full Length Article

Numerical analysis of friction factor for a fully developed turbulent flow using k–ε turbulence model with enhanced wall treatment

Muhammad Ahsan *

School of Chemical & Materials Engineering, National University of Sciences & Technology, Islamabad 44000, Pakistan

ARTICLE INFO

Article history:
Received 22 March 2014
Accepted 7 November 2014
Available online 6 December 2014

Keywords:
Turbulent flow
Enhanced wall treatment
k–ε turbulence model
Computational fluid dynamics (CFD)
Friction factor

ABSTRACT

The aim of this study is to formulate a computational fluid dynamics (CFD) model that can illustrate the fully turbulent flow in a pipe at higher Reynolds number. The flow of fluids in a pipe network is an important and widely studied problem in any engineering industry. It is always significant to see the development of a fluid flow and pressure drop in a pipe at higher Reynolds number. A finite volume method (FVM) solver with k–ε turbulence model and enhanced wall treatment is used first time to investigate the flow of water at different velocities with higher Reynolds number in a 3D pipe. Numerical results have been presented to illustrate the effects of Reynolds number on turbulence intensity, average shear stress and friction factor. Friction factor is used to investigate the pressure drop along the length of the pipe. The contours of wall function are also presented to investigate the effect of enhanced wall treatment on a fluid flow. A maximum Reynolds number is also found for which the selected pipe length is sufficient to find a full developed turbulent flow at outlet. The results of CFD modeling are validated by comparing them with available data in literature. The model results have been shown good agreement with experimental and co-relation data.

1. Introduction

In a field of fluid dynamics and heat transfer turbulent flow over rough surfaces has been a topic of increasing interest. This type of flow can be observed in various engineering applications such as heat exchangers, nuclear reactor, turbine blade, wind tunnel, fluid catalytic cracking and air foil (Ahsan, 2012; Aly and Bitsuamlak, 2013; Aly, 2014). Other examples of relevance have been mentioned by Pimentel et al. (1999). A study in pipe flow to observe the effects of relative roughness and Reynolds number on velocity distribution and friction factor was performed by Bradshaw (2000). The work concluded that the relation between velocity distribution and resistance formula could be extended from smooth pipes to rough pipes (Singh and Makinde, 2012). Many experimental

* Tel.: +92 3336057937.
E-mail address: ahsan@scme.nust.edu.pk.
Peer review under the responsibility of Beni-Suef University.
http://dx.doi.org/10.1016/j.bjbas.2014.12.001

studies have been completed to get the knowledge about velocity distribution, pressure drop and turbulent flow behavior near rough walls (Reif and Andersson, 2002; Majumdar and Deb, 2003; Vijiapurapu and Cui, 2007; 2010). Several studies have been performed to investigate the heat transfer as a function of roughness height to hydraulic diameter, spacing between Reynolds number and roughness elements (Fabbri, 2000; Togun et al., 2011; Zhang et al., 2011). The comparison between rib pitch and rib height with roughness of sand was carried by various researchers (Wang et al., 2004; Di Nucci and Russo Spena, 2012).

In rough pipes the inspection of fluctuating velocity spectra is used to find the turbulence profile in all coordinate directions. A significant observation of this study was that the nature of the solid boundary has negligible effect on the flow in the central part of the pipe. On the other hand the flow near the wall is dependent on the nature of the solid boundary (Rao and Kumar 2009). In literature different approaches were proposed by several researchers to study the relationship of turbulent flow and rough surfaces. The behavior of turbulent flow in ducts by implementing roughness element drag coefficient is studied by Wang et al. (2004). Kandlikar et al. (2005) experimentally determined the repeated-rib roughness in tubes. Recently formula for the mean velocity calculation across the inner layer of turbulent boundary is proposed (Scibilia, 2000). The velocity profile obtained by busing this formula is used to formulate the friction factor correlation for the fully developed turbulent pipe flow. Saleh (Di Nucci and Russo Spena, 2012) observed the effects of roughness by using k–ε turbulence model in conjunction with empirical wall function. Other significant works with the implementation of k–ε turbulence model were studied by Cardwell et al. (2011) and Walker (2005). Different approach was proposed by Johansen et al. (2003), Pinson and Wang (1999), Zimparov (2004)and Zhu and Kuznetsov (2005) to study the influence of the rough wall by using the modified mixed length model. They also proposed the solution for external and internal flow fields in pipe. The advantage of using this approach is reduction in computation cost as compared to other approaches. k–ε model can be used with moderate roughness with in a suitable degree of accuracy. The researchers concluded that the k–ε model with enhanced wall treatment among different turbulence models gives the most suitable prediction.

The present study deals with the CFD analysis of fully developed turbulent flow in a 3D pipe using k–ε turbulence model with enhanced wall treatment. Moreover a maximum Reynolds number is predicted which is sufficient to obtain a fully developed flow for a current pipe length at outlet. The contours of wall function are also shown to see the effect of enhanced wall treatment. This paper also illustrates the effects of Reynolds number, inlet velocity and wall shear stress on a friction factor. The predicted friction factor is compared to the experimental values in order to validate the results. The schematic pipe used in this study is shown in Fig. 1.

2. Mathematical modeling

2.1. Governing equations

The continuity equation in differential form is

$$\frac{\partial \rho}{\partial t} + \nabla \cdot (\rho \vec{v}) = S_m \tag{1}$$

Conservation of momentum in an inertial (non-accelerating) reference frame is described by Batchelor (2000)

$$\frac{\partial}{\partial t}(\rho \vec{v}) + \nabla \cdot (\rho \vec{v} \vec{v}) = -\nabla p + \nabla \cdot (\bar{\bar{\tau}}) + \rho \vec{g} + \vec{F} \tag{2}$$

2.2. Turbulence model

The two equations model is most simple and famous turbulence model. In this model the length scales and turbulent velocity are calculated independently by using the solution of different transport equations. The standard k–ε model has become the widely used turbulence model for the solution of practical engineering flow problems (Rolander et al., 2006). Such model is a semi-empirical model built on model transport equations for the turbulence kinetic energy k and its dissipation rate ε. The model transport equation for k is derived from the exact equation, while the model transport equation for ε was obtained using physical reasoning and bears little resemblance to its mathematically exact counterpart (FLUENT, 2006).

2.2.1. Transport equations for the standard k–ε model

$$\frac{\partial}{\partial t}(\rho k) + \frac{\partial}{\partial x_i}(\rho k u_i) = \frac{\partial}{\partial x_j}\left[\left(\mu + \frac{\mu_t}{\sigma_k}\right)\frac{\partial k}{\partial x_j}\right] + G_k + G_b - \rho\varepsilon - Y_M + S_k \tag{3}$$

and

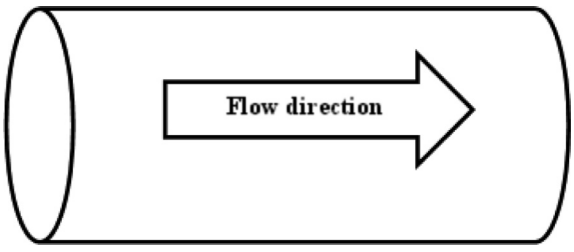

Fig. 1 – Schematic of fluid flow in a pipe.

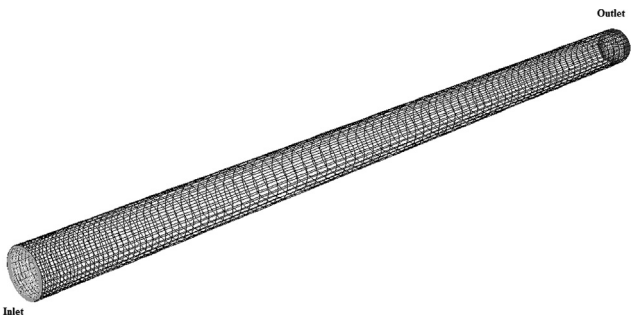

Fig. 2 – Computational grid of 3D pipe.

$$\frac{\partial}{\partial t}(\rho\varepsilon)+\frac{\partial}{\partial x_i}(\rho\varepsilon u_i)=\frac{\partial}{\partial x_j}\left[\left(\mu+\frac{\mu_t}{\sigma_\varepsilon}\right)\frac{\partial \varepsilon}{\partial x_j}\right]+C_{1\varepsilon}\frac{\varepsilon}{k}\left(G_k+C_{3\varepsilon}G_b\right)-C_{2\varepsilon}\rho\frac{\varepsilon^2}{k}+S_\varepsilon \quad (4)$$

2.2.2. Modeling the turbulent viscosity

$$\mu_t=\rho C_\mu\frac{k^2}{\varepsilon} \quad (5)$$

2.2.3. Model constants

The model constants $C_{1\varepsilon}$, $C_{2\varepsilon}$, C_μ, σ_k and σ_ε have the following default values (Rolander et al., 2006)

$C_{1\varepsilon}=1.44,\ C_{2\varepsilon}=1.92,\ C_\mu=0.09,\ \sigma_k=1.0,\ \sigma_\varepsilon=1.3$

These default values have been determined from experiments with air and water for fundamental turbulent shear flows comprising homogeneous shear flows and decaying isotropic grid turbulence. They have been found to work equally fine for an inclusive range of wall-bounded and free shear flows.

2.3. Enhanced wall treatment

Enhanced wall treatment is a near-wall modeling method that combines a two-layer model with enhanced wall functions. Precisely, in k–ε model enhanced wall treatment is the methodology of combining different wall functions. This is why it is also called two layer approach. It is used one equation relationship to evaluate the laminar sub-layer with fine mesh and transition to log-low function for the turbulent part of the boundary layer. The utilization of y+ with enhanced wall treatment provides these scalable advantages over the standard wall functions. The restriction that the near-wall mesh must be suitably fine everywhere might impose too large a computational requirement.

2.3.1. Two-layer model for enhanced wall treatment

In the near-wall model, the viscosity-affected near-wall region is entirely determined all the way to the viscous sub-layer. The two-layer method is an integral part of the enhanced wall treatment and is used to specify both ε and the turbulent viscosity in the near-wall cells. The separation of the two regions is expressed by a wall-distance-based, turbulent Reynolds number, Re_y, defined as (FLUENT, 2006).

$$Re_y\equiv\frac{\rho y\sqrt{k}}{\mu} \quad (6)$$

$$y\equiv\min_{\vec{r}_w\,\varepsilon\Gamma_w}\left\|\vec{r}-\vec{r}_w\right\| \quad (7)$$

This explanation permits y to be exclusively explained in flow domains of complex shape including multiple walls. Additionally, y defined in such a way is independent of the mesh topology used, and is definable even on unstructured meshes.

2.3.2. Enhanced wall functions

To have a method that can spread its applicability all over the near-wall region (i.e. laminar sub-layer, buffer region, and fully-turbulent outer region) it is essential to develop the law of the wall as a single wall law for the whole wall region. Model reaches this by joining together linear (laminar) and logarithmic (turbulent) laws-of-the-wall using a function (Motozawa et al., 2012).

$$u^+=e^{\Gamma}u^+_{lam}+e^{\frac{1}{\Gamma}}u^+_{turb} \quad (8)$$

$$\Gamma=\frac{a(y^+)^4}{1+by^+} \quad (9)$$

Where a = 0.01 and b = 5. Similarly, the common equation for the derivative du^+/dy^+ is

$$\frac{du^+}{dy^+}=e^{\Gamma}\frac{du^+_{lam}}{dy^+}+e^{\frac{1}{\Gamma}}\frac{du^+_{turb}}{dy^+} \quad (10)$$

Where e is the natural logarithm constant, this methodology permits the fully turbulent law to be simply improved and extended to determine the effects such as variable properties or pressure gradients. This formula also guarantees the right asymptotic behavior for small and large values of y+ and acceptable illustration of velocity profiles in the problems where y+ lies inside the wall buffer region ($3 < y+ < 10$).

2.4. Friction factor and basic equations

The Reynolds number is defined as $Re = \rho uD/\mu$, the Turbulence intensity (T.I) is calculated by $T.I = 0.16 \times Re^{-1/8}$. Friction factor (*f*) is used to show the pressure drop in a pipe for turbulent flow (Chao et al., 2007). It is defined as

$$f=\frac{2\Delta PD}{L\rho v^2} \quad (11)$$

After balancing the pressure and shear forces the same expression takes the form:

$$f=\frac{8\tau_w}{\rho v^2} \quad (12)$$

This expression is known as Darcy friction factor (de Lima et al., 2012). Head loss for fully developed flow is determined by co-relation

$$H_l=fLv^2/2Dg \quad (13)$$

3. Simulation setup and numerical discretization

The geometry of the pipe is shown in Fig. 1. The water enters into a pipe with a specific velocity. The pipe total length of a pipe is 20 m with diameter of 1 m. GAMBIT™ pre-process was used to construct the 3D pipe. Hexahedral grids were used throughout. The density of water was 1000 kg/m^3 and viscosity about 0.001 kg/m s. The velocity of water at the inlet varied from 0.010, 0.015, 0.020, 0.025, 0.030, 0.035 and 0.040 m/s. At the outlet, pressure outlet condition is applied to the pipe. Steady and incompressible flow of water is considered in this analysis (see Fig. 2).

The 3D geometry is discretized using 39,870 rectangular cells. Grid size analysis is carried out using three different

mesh intervals, i.e. 1 mm, 2 mm and 3 mm. All the simulation results did not show any major difference. The solution procedure adopted to solve the CFD model using FVM solver is shown in Fig. 3.

The default solver setting are selected because pressure based solver is used to solve the steady state problem. An atmospheric pressure is maintained at outlet therefore use default value (0 Pa for gage pressure). The governing equations are solved using the finite-volume method. In these calculations, the second order upwind scheme based on multidimensional linear reconstruction approach is used (Tan et al., 2012).

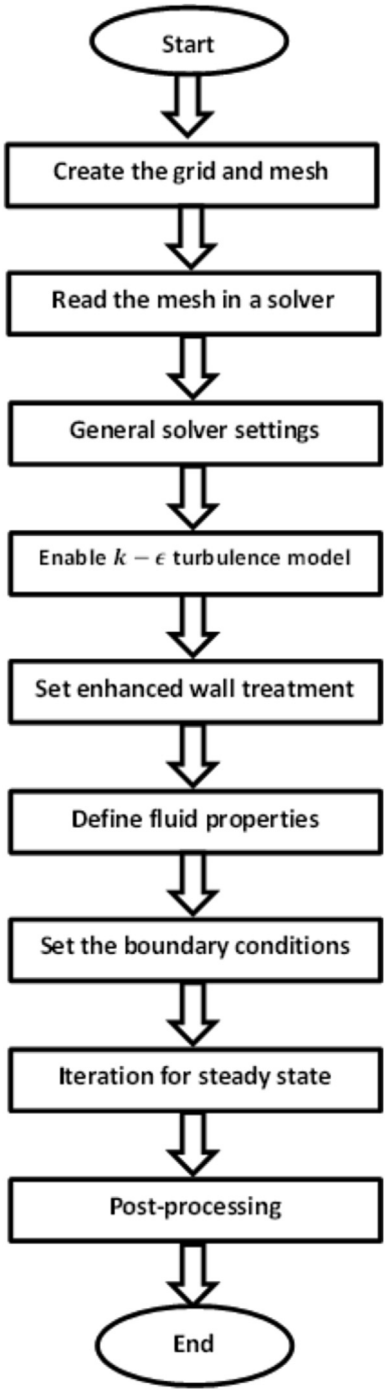

Fig. 3 – Solution procedure for CFD model.

Higher order discretization schemes can be apply directly because the flow is not very complex.

It is suggested to solve complex flows problems with first order schemes before implementing higher order schemes. In this method, higher-order accuracy is attained at cell faces through a Taylor series expansion of the cell-centered solution about the cell centroid. The SIMPLE algorithm for pressure–velocity coupling with second order upwind discretization scheme is used to obtain solution for the equations of Momentum, Turbulence Kinetic Energy and Turbulence Dissipation Rate. The target of all discretization techniques in FVM is to develop a mathematical model to convert each of terms into an algebraic equation. Once implemented to complete control volumes in a particular mesh, we attain a full linear system of equations that requires to be solved. These computations are carried out using FVM solver (ANSYS FLUENT™) (FLUENT, 2006), a commercial CFD package with a 3D double precision configuration. Simulation is carried on an Intel Dual Core Microsystems™ with 32 bit processor and 1 GB RAM.

There is no fix criterion for the evaluation of convergence. Residual definition varies with the nature of the problem. For most problems, the default convergence criterion in FLUENT is sufficient. This criterion requires that the scaled residuals decrease to 10^{-3} for all equations except the energy and radiation equations, for which the criterion is 10^{-6}. In order to predict the results more sufficiently in this simulation the residuals decrease to 10^{-6} (FLUENT, 2006). In steady state solutions for various Reynolds number have been converged within 300 iterations.

4. Results and discussion

In this study, simulations were performed to investigate the effect of Reynolds Number on turbulence intensity, shear stress and friction factor. More over the maximum Reynolds number is also determined to obtain a fully developed turbulent flow for current pipe length.

Fig. 4 shows the velocity profiles in the pipe at different Reynolds numbers. These profiles determined the length at which the flow is fully developed for different Reynolds

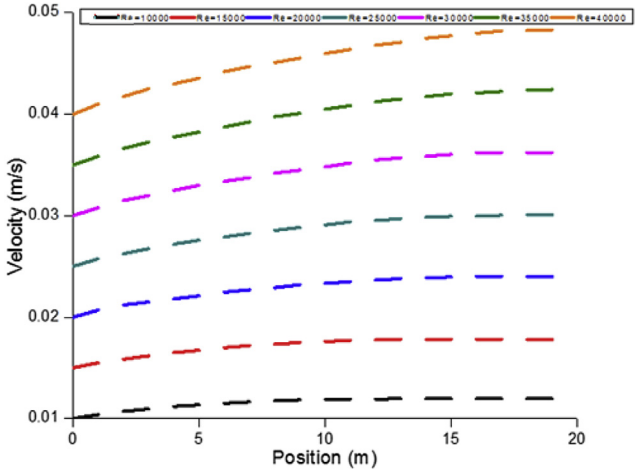

Fig. 4 – Velocity profiles in the pipe at different Reynolds number.

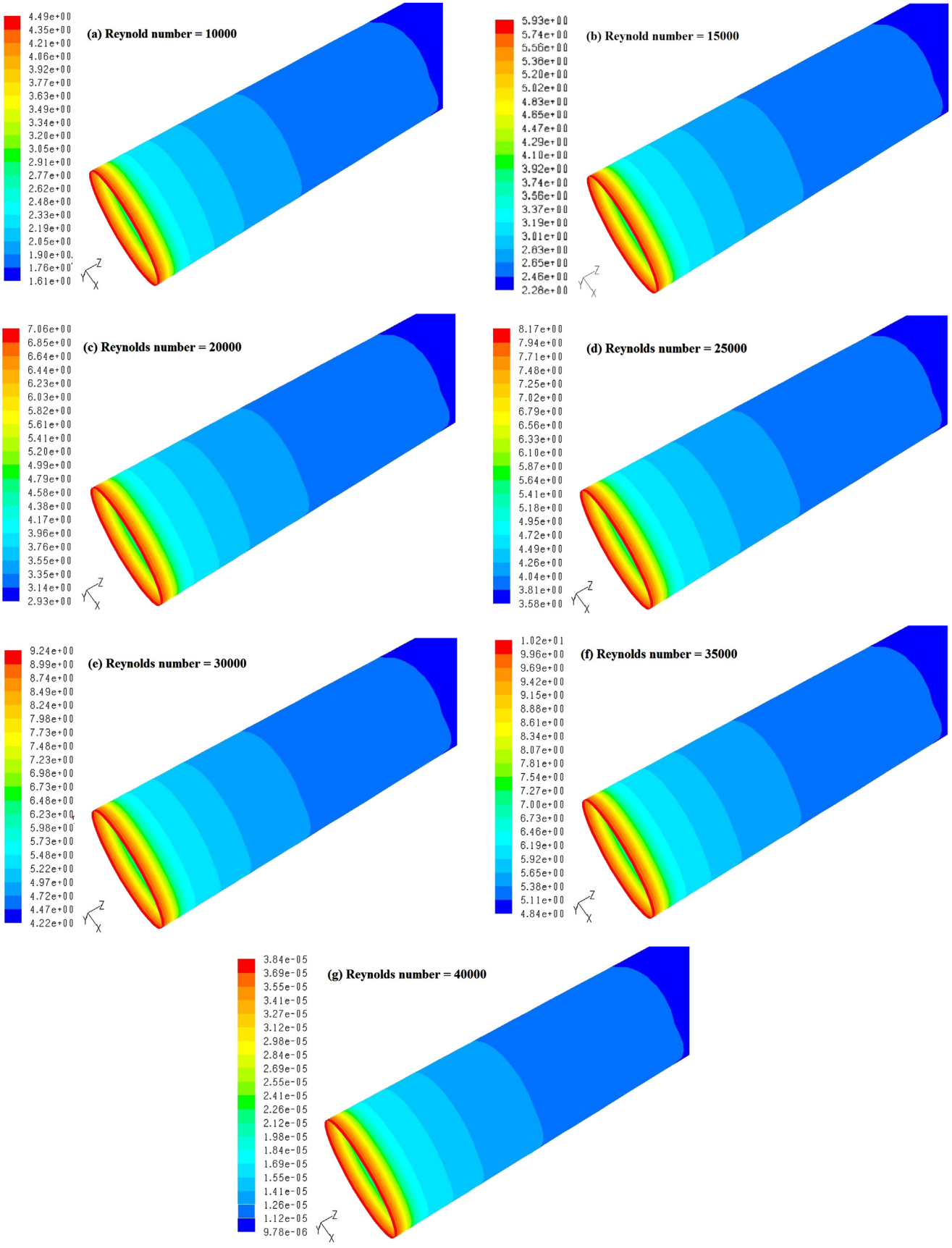

Fig. 5 – (a)–(g) Contours of Wall Y plus function at various Reynolds numbers.

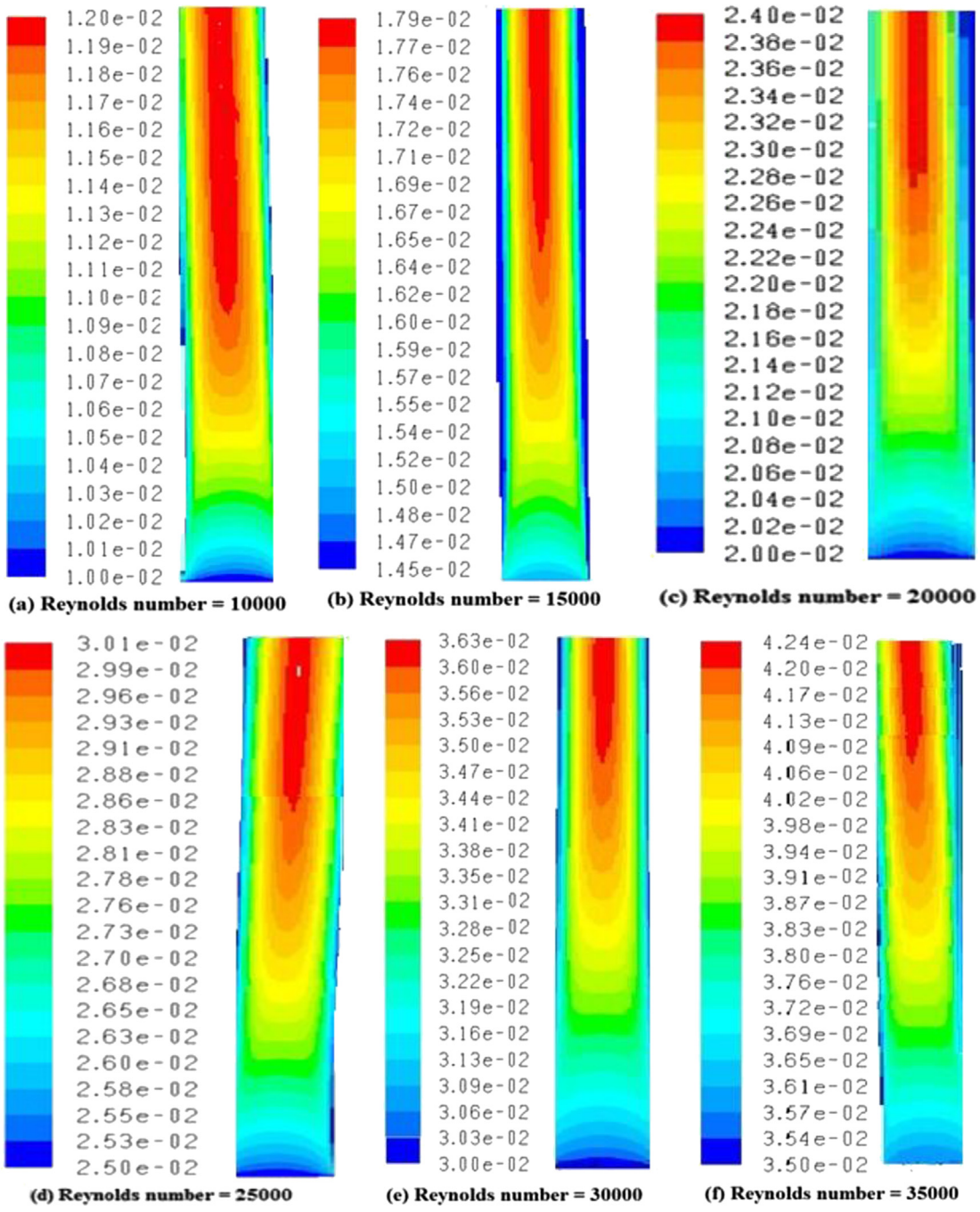

Fig. 6 – (a)–(f) Contours of velocity magnitude (m/s) at various Reynolds numbers.

number. The turbulent flow is fully developed for Reynolds numbers from 10,000 to 30,000. For Reynolds numbers 35,000 and 40,000 the flow has started to fully develop just before reaching the outlet of a pipe. The entry length of the pipe could be measured by using these profiles. The entry length is defined as the distance along the pipe length where velocity reaches 99.9% of its final value. We can observed that the entry length values appears to be 15 m, which shows good similarity with values described in literature (Çengel et al., 2012).

Fig. 5(a)–(g) shows the contours of wall Y-plus function. The Y-plus value for maximum of the domain is less than 10, except for the cells near inlet, where it is marginally higher. This displays that enhanced wall treatment is adequate as a wall function. The highest value of wall Y plus function rises with increasing Reynolds number.

Fig. 6(a)–(f) describes the contours of velocity magnitude at different Reynolds numbers. We can observe the variation in the velocity of a fluid in a pipe along the Z-axis.

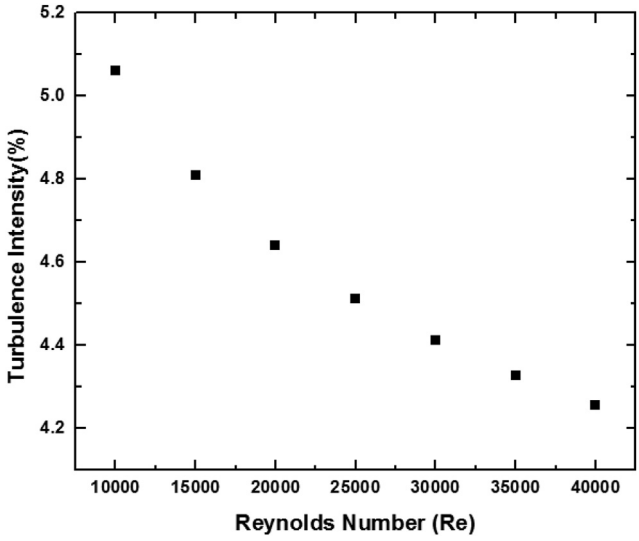

Fig. 7 – Effect of changing Reynolds number on the turbulence intensity.

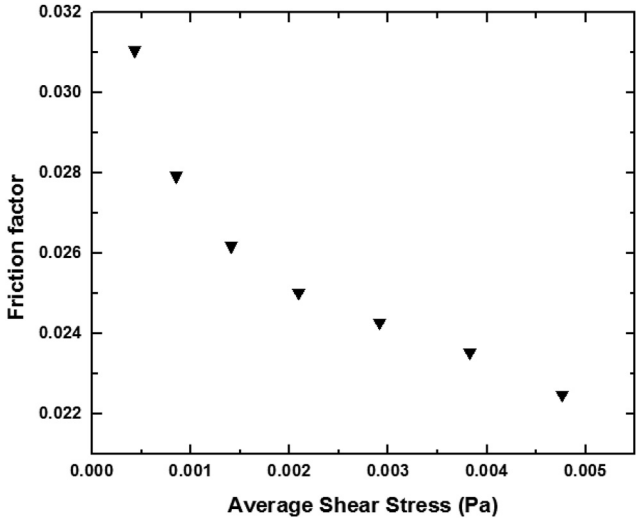

Fig. 9 – Average shear stress vs friction factor.

In Fig. 7 effect of different Reynolds number on the turbulence intensity has been illustrated, the turbulence intensity decreases with the increase in Reynolds number. These values of turbulence parameters are normally be used if reverse flow occurs at the outlet.

Fig. 8 predicts the increase in the average shear stress on the wall of a pipe as the Reynolds number increase. An iso-surface is created in Z-coordinate and surface integrals of wall shear stress for are calculated on this surface. We conclude that the Reynolds number and average shear stress are related directly to each other.

Fig. 9 shows the relation between friction factor and average shear stress. The value of bulk velocity is obtained from FVM solver and put in equation (12) to calculate the friction factor for various Reynolds numbers. The model predicts the decrease in the friction factor as the average shear stress increases.

Fig. 10 depicts the effect of changing Reynolds number on friction factor. The friction factor decreases as the Reynolds number increase, which is correspondence with the friction factor determined from co-relation reported in literature (Moody, 1944).

Table 1 shows the comparison of head loss of this model with the results obtained by co-relation shown in equation (13). The difference between the co-relation values and simulation results are negligible. We can utilize the simulation results obtained from the CFD model to determine the other fluid characteristics efficiently. To summarize the preceding discussion, we see that as Reynolds number is increasing the friction factor decreases gradually and finally the values will level out at a constant value for large Reynolds number. CFD analysis is implanted to examine the hydrodynamics of a problem accurately at higher Reynolds number.

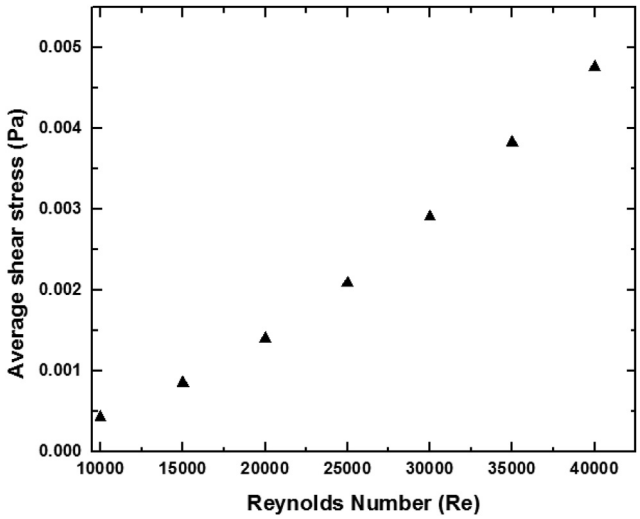

Fig. 8 – Average shear stress vs Reynolds number.

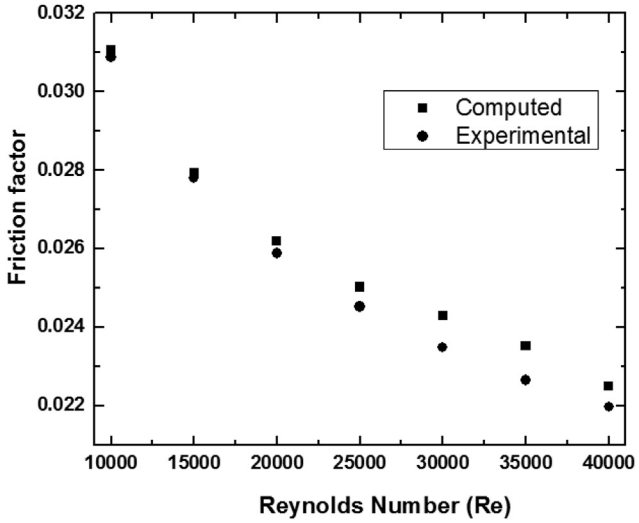

Fig. 10 – Average shear stress vs friction factor.

Table 1 – Comparison of head loss in this work with co-relation.

Velocity (m/s)	Head loss [this model]	Head loss [co-relation]	% Difference
0.010	0.000334703	0.000332691	0.60
0.015	0.000666083	0.000662879	0.48
0.02	0.00110107	0.001088384	1.16
0.025	0.00163702	0.0016041	2.03
0.030	0.002281783	0.002206522	3.35
0.035	0.003002964	0.002890919	3.80
0.040	0.003734905	0.003648788	2.33

5. Conclusions

The extrapolative abilities of k–ε turbulence model have been tested as they implemented to the calculation of fully developed turbulent flow in a 3D pipe with enhanced wall treatment. The k–ε model with high Reynolds numbers has been implemented to calculate the fluid velocities and pressure drop using friction factor. This model has been used to predict the various aspects of the fluid flow in a pipe, including the behavior of wall Y plus function at various Reynolds numbers, effects of Reynolds number on turbulence intensity, average shear stress and friction factor. Pressure drops for fully developed flow of fluid through pipe could be predicted using this model. The foretelling capability of the k–ε model is likely to improve when the enhanced wall treatment is included in the model. The advantage of using k–ε turbulence model is that it's computationally cheap. This study shows that CFD model is in good agreement with the results reported in the literature. This model can be extended by implementing large eddy simulation (LES) and direct numerical simulation (DNS) models to a 3D geometry with fewer assumptions. This model can be used to for the determination of heat transfer through a 3D pipe by including energy equation in the model.

Nomenclature

ρ	Fluid density, static pressure (Eq. (2))
t	Time
$\vec{v}$	Flow velocity vector field
S_m	Mass added to the continuous phase from the dispersed second phase
$\bar{\bar{\tau}}$	Stress tensor
$\rho\vec{g}$	Gravitational body force
$\vec{F}$	External body forces
k	Turbulence kinetic energy
ε	Rate of dissipation
G_k	Generation of turbulence kinetic energy due to the mean velocity gradients
G_b	Generation of turbulence kinetic energy due to buoyancy,
Y_M	Contribution of the fluctuating dilatation in compressible turbulence to the overall dissipation rate,
$C_{1\varepsilon}$, $C_{2\varepsilon}$, $C_{3\varepsilon}$, C_μ	Constants
σ_k	Turbulent Prandtl numbers for k
σ_ε	Turbulent Prandtl numbers for ε
S_k, S_ε	user defined source terms
μ_t	Turbulent (or eddy) viscosity
y	Normal distance from the wall at cell centers
$\vec{r}$	Position vector at the field
$\vec{r_w}$	Position vector on the wall boundary
Γ_w	Union of all the wall boundaries involved
Γ	Blending function
u	velocity of the fluid
D	Diameter of the pipe
μ	Viscosity of the fluid
ΔP	Pressure drop along pipe length
v	average velocity in the pipe section,
L	length of the pipe
τ_w	Shear stress on the wall
g	Gravity

REFERENCES

Ahsan M. Computational fluid dynamics (CFD) prediction of mass fraction profiles of gas oil and gasoline in fluid catalytic cracking (FCC) riser. Ain Shams Eng J 2012;3(4):403–9.

Aly AM. Atmospheric boundary-layer simulation for the built environment: past, present and future. Build Environ 2014;75:206–21.

Aly AM, Bitsuamlak G. Aerodynamics of ground-mounted solar panels: test model scale effects. J Wind Eng Ind Aerodyn 2013;123:250–60.

Batchelor GK. An introduction to fluid dynamics. Cambridge University Press; 2000.

Bradshaw P. A note on "critical roughness height" and "transitional roughness". Phys Fluids 2000;12:1611.

Cardwell ND, Vlachos PP, Thole KA. Developing and fully developed turbulent flow in ribbed channels. Exp Fluids 2011;50(5):1357–71.

Çengel YA, Turner RH, Cimbala JM. Fundamentals of thermal-fluid sciences with student resource dvd. McGraw-Hill; 2012.

Chao DA, Castillo L, Turan ÖF. Effect of roughness in the development of an adverse pressure gradient turbulent boundary layer. 2007. 16th Australasian Fluid Mechanics Conference (AFMC), School of Engineering, The University of Queensland.

de Lima A, Neto SF, Silva W. Heat and mass transfer in porous materials with complex geometry: fundamentals and applications. Heat and mass transfer in porous media. Springer; 2012. p. 161–85.

Di Nucci C, Russo Spena A. Mean velocity profiles of two-dimensional fully developed turbulent flows. C R Mec 2012;340(9):629–40.

Fabbri G. Heat transfer optimization in corrugated wall channels. Int J Heat Mass Transf 2000;43(23):4299–310.

FLUENT A. ANSYS FLUENT user guide manual. 2006.

Johansen S, Skalle P, Sveen J. A generic model for calculation of frictional losses in pipe and annular flows. J Can Pet Technol 2003;42(6).

Kandlikar SG, Schmitt D, Carrano AL, Taylor JB. Characterization of surface roughness effects on pressure drop in single-phase flow in minichannels. Phys Fluids 2005;17:100606.

Majumdar P, Deb P. Computational analysis of turbulent fluid flow and heat transfer over an array of heated modules using turbulence models. Numer Heat Transf A Appl 2003;43(7):669–92.

Moody LF. Friction factors for pipe flow. Trans ASME 1944;66(8):671–84.

Motozawa M, Ishitsuka S, Iwamoto K, Ando H, Senda T, Kawaguchi Y. Experimental investigation on turbulent structure of drag reducing channel flow with blowing polymer solution from the wall. Flow Turbul Combust 2012;88(1–2):121–41.
Pimentel L, Cotta R, Kakac S. Fully developed turbulent flow in ducts with symmetric and asymmetric rough walls. Chem Eng J 1999;74(3):147–53.
Pinson MW, Wang T. Effect of two-scale roughness on boundary layer transition over a heated flat plate: part 2—boundary layer structure. J Turbomach 1999;122(2):308–16.
Rao AR, Kumar B. Transition of turbulent pipe flow. J Hydraul Res 2009;47(4):529–33.
Reif BP, Andersson H. Prediction of turbulence-generated secondary mean flow in a square duct. Flow Turbul Combust 2002;68(1):41–61.
Rolander N, Rambo J, Joshi Y, Allen JK, Mistree F. An approach to robust design of turbulent convective systems. J Mech Des 2006;128:844.
Scibilia M-F. Heat transfer in a forced wall jet on a heated rough surface. J Therm Sci 2000;9(1):85–92.
Singh G, Makinde OD. Computational dynamics of MHD free convection flow along an inclined plate with Newtonian heating in the presence of volumetric heat generation. Chem Eng Commun 2012;199(9):1144–54.
Tan X-H, Zhu D-S, Zhou G-Y, Zeng L-D. Experimental and numerical study of convective heat transfer and fluid flow in twisted oval tubes. Int J Heat Mass Transf 2012;55(17):4701–10.
Togun H, Kazi S, Badarudin A. A review of experimental study of turbulent heat transfer in separated flow. Aust J Basic Appl Sci 2011;5(10):489–505.
Vijiapurapu S, Cui J. Simulation of turbulent flow in a ribbed pipe using large eddy simulation. Numer Heat Transf A Appl 2007;51(12):1137–65.
Vijiapurapu S, Cui J. Performance of turbulence models for flows through rough pipes. Appl Math Model 2010;34(6):1458–66.
Walker P. CFD modelling of heat exchanger fouling. University of New South Wales Sydney Australia; 2005.
Wang Z, Chi X, Shih T, Bons J. Direct simulation of surface roughness effects with RANS and DES approaches on viscous adaptive Cartesian grids. 2004. AIAA Paper 2420.
Zhang Z, Lowe R, Falter J, Ivey G. A numerical model of wave-and current-driven nutrient uptake by coral reef communities. Ecol Model 2011;222(8):1456–70.
Zhu J, Kuznetsov A. Forced convection in a composite parallel plate channel: modeling the effect of interface roughness and turbulence utilizing a k–ε model. Int Commun Heat Mass Transf 2005;32(1):10–8.
Zimparov V. Prediction of friction factors and heat transfer coefficients for turbulent flow in corrugated tubes combined with twisted tape inserts. Part 1: friction factors. Int J Heat Mass Transf 2004;47(3):589–99.